Early Stopping Criterion for Recursive Least Squares Training of Behavioural Models

Meabh Loughman (meabh.loughman.2018@mumail.ie)
Maynooth University: National University of Ireland Maynooth https://orcid.org/0000-0001-8901-2937
Sinead Barton
Maynooth University: National University of Ireland Maynooth
Ronan Farrell
Maynooth University: National University of Ireland Maynooth
John Dooley
Maynooth University: National University of Ireland Maynooth

Research Article

Keywords: Behavioural modeling , Power Amplifier , Recursive least squares (RLS) , Volterra Model

DOI: https://doi.org/10.21203/rs.3.rs-452849/v1

Wireless Personal Communications manuscript No.
(will be inserted by the editor)

Early Stopping Criterion for Recursive Least Squares Training of Behavioural Models

Méabh Loughman, Sinéad Barton, Ronan Farrell · John Dooley

Received: date / Accepted: date

Abstract As the physical makeup of cellular base-stations evolve into systems with multiple parallel transmission paths the effort involved in modelling these complex systems increases considerably. One task in particular which contributes to signal distortion on each signal path, is the power amplifier. In power amplifier modelling, Recursive Least Squares has been used in the past to train Volterra models with memory terms, however instability can occur when training the model weights. This manuscript provides a computationally efficient technique to detect the onset of instability and subsequently to inform the decision when to stop adaptive training of dynamic nonlinear behavioural models and avoid the onset of instability. This technique is experimentally validated using four different signal modulation schemes.

Keywords Behavioural modeling · Power Amplifier · Recursive least squares (RLS) · Volterra Model

1 Introduction

Radio transceivers are increasing in complexity as a result of a more demanding and technology driven population [1]. Power amplifiers (PAs) are a crucial component in the architecture of a transceiver chain, responsible for increasing the power of a signal to ensure accurate and reliable transmission. Historically, PAs are first required to operate with linear behaviour, however, as the drive to improve power efficiency increases a compromise must be met between linearity and efficiency. Distributed arrays of PAs are needed for many of the proposed architectures for future wireless networks. Behavioural modelling of PAs is an essential technique for high level testing of PA behaviours under various circumstances.

This publication has emanated from research conducted with the financial support of Science Foundation Ireland (SFI) and is co-funded under the European Regional Development Fund under Grant Number 13/RC/2077.

Department of Electronic Engineering Maynooth University
Co. Kildare
Ireland
E-mail: meabh.loughman.2018@mumail.ie

Extracting accurate models reduces the cost of hardware implementation testing. One major objective in behavioural modelling RF systems is to identify the most computationally efficient structure that can accurately characterise the behaviour.

The primary objective of this paper was to combine the Volterra Model and RLS error correction in order to identify an early stopping criterion for use during training of the PA model. The Volterra model and RLS error correction were chosen due to their combined propensity for instability during training. Experimental analysis was conducted to determine and implement the early stopping criteria in this context.

The Volterra series [2] [3] [4] calculates each interaction of its inputs up to a defined order of non-linearity. As the number of inputs or the order of non-linearity increases, the number of coefficients increases rapidly and therefore increases the computational complexity [5]. Although the computational complexity is increased the Volterra Model is capable of accurately describing non linear systems with memory [6]. Recursive Least Squares (RLS) is an iterative form of least mean squares that is more rapid in converging to the minimum error while training a model [7] [8]. Using RLS without limiting the input training signal length can lead to instability during training [9].

Work demonstrated by [10] alters the RLS algorithm to decrease error by incorporating a variable forgetting factor and convergence factor to implement a look up table for an adaptive digital pre distortion technique. Authors of [11] focus on alternative Volterra models to reduce NMSE for PA behavioural modeling. However, increased accuracy results in increased computational complexity and may still result in an unstable model.

Previous papers have demonstrated alternative methods to maintain stability during training using the RLS algorithm. Authors in [12], demonstrated that altering the recursive least squares algorithm to include periodic regularisation and maximum and minimum eigenvalue limitations can help to maintain stability. Additionally it was reported in [12] that this causes a slight degradation in dynamic range and requires stricter variable thresholding. Authors of [13] alter the RLS algorithm by adapting a hybrid approach of directional and exponential forgetting factorisation to implement an adaptive forgetting factor. Disparate accuracy of the proposed method is reported when comparing results using two different PAs. The results are also highly dependent on *a priori* data. In [14] two computations of DPD coefficients are performed, with one set of coefficients specifically containing peaks. The computational complexity introduced by needing to compute two sets of DPD coefficients leads to a less attractive solution. In [12], [13], and [14] all propose techniques that require additional computations in order to maintain the stability during training. In this work a computationally efficient approach is presented to avoid the onset of instability during model coefficient training for the RLS algorithm.

The remainder of the paper is organised as follows: Sections 2 and 3 provides an outline of Volterra modeling and conventional RLS algorithm respectively. In Section 4 the early stopping criteria is introduced and justified. Experimental measurements are presented for the validation of the approach in 5 and finally the results and conclusions from the work are outlined in Section 5.

2 The Volterra Model

PAs are important components of signal transmission chains as they are responsible for increasing the power of the communication signals to power levels that are suitable for transmission. PAs are typically one of the last components in the radio transmitter chain and thus, handle a considerable measure of power, the efficiency at which PAs convert DC power into RF power is a critical role on the overall power consumption of transceiver infrastructure.

PAs exhibit non linear behaviour, causing signal distortion in transmission. A signal sent through a PA will experience distortion at different power levels, dependant on what PA architecture is utilised and the signal envelope variation [15]. Ideally, PAs should operate with a high power output and illicit linear behaviour.

Digital predistortion (DPD) is a technique that illicits linear behaviour of the PA by altering the magnitude and phase of an input signal. In order for DPD to create a complimentary or inverse function to eliminate non linearities introduced by a PA, behavioural modelling is used.

Behavioural modeling using the Volterra series combines numerous linear convolutions and a non linear power series, allowing the system to be modelled while incorporating memory effects [4]. Although the accuracy of the Volterra model is high the computational complexity is also high as the number of parameters to be estimated escalates rapidly as the non linear order of the model and the memory depth heightens.

A system with finite order of non-linearity with finite memory depth can be described in the time domain by equation 1.

$$y(n) = \sum_{p=1}^{P} y_p(n) \tag{1}$$

Where,

$$y_p(n) = \sum_{i_1=0}^{N-1} \cdots \sum_{i_P=0}^{N-1} h_p(i_1, \cdots, i_p) \prod_{i=1}^{p} x(n - i_r)$$

Where $x(n)$ and $y(n)$ is the input and output signal to the system respectively. $h_p(i_1, ..., ip)$ represents the filter co-efficient expansion utilising, p, the highest order for the non-linearity of the Volterra series expansion. N represents the maximum memory tap length chosen [16].

3 Theory of Conventional Recursive Least Squares (RLS) Training Algorithm

RLS is a well known training method used for training the behavioural models of PAs [7] [8]. However, RLS has a tendency to produce unstable models. Previous literature to the best of the authors knowledge has not identified a factor that can predict the point at which the training routine will become unstable. The following mathematical analysis provides a method to predict and constrain training to prevent instability occurring.

The exponentially weighted RLS algorithm can be adequately described in terms of its cost function. Model coefficients (in this case specifically referring to the Volterra model), are adapted based on the cost function $J(n)$, shown below in equation 2.

$$J(n) = \sum_{k=1}^{n} \lambda^{(n-k)} (d(k) - \overrightarrow{\boldsymbol{H}}^T(n)\boldsymbol{X}(k))^2 \tag{2}$$

λ is an exponentially weighted factor, $0 < \lambda < 1$, controlling the convergence speed of the function, referred to here, as the forgetting factor. λ closer to 1 enables the algorithm to decay slowly, tracking signal alterations more closely. The inverse is true for λ tending to 0. $d(k)$, refers to the actual output signal at sample k.Filter coefficients, $\overrightarrow{\boldsymbol{H}}(n)$, are determined such that the weighted average of the squared estimation error is minimised from time $k = 1$ to $k = n$. [9]. $\boldsymbol{X}(k)$ represents the input signal to the model at sample k.

The following equations give a mathematical description of the RLS algorithm to minimise the cost function in equation 2 by minimising the error ε to update $\overrightarrow{\boldsymbol{H}}(n)$ and the update matrix $\boldsymbol{C}^{-1}(n)$ in an iterative fashion , heuristically as in the conventional RLS algorithm [9] where $K(n)$ depicts the gain vector.

$$\varepsilon(n) = d(n) - \boldsymbol{X}^T(n)\boldsymbol{H}(n-1) \tag{3}$$

$$K(n) = \boldsymbol{C}^{-1}(n)\boldsymbol{X}(n) \tag{4}$$

$$\boldsymbol{C}^{-1}(n) = \frac{\boldsymbol{C}^{-1}(n-1)}{\lambda} - \frac{K(n)\boldsymbol{X}^T(n)\boldsymbol{C}^{-1}(n-1)}{\lambda} \tag{5}$$

$$\boldsymbol{H}(n) = \boldsymbol{H}(n-1) + K(n)\varepsilon(n) \tag{6}$$

Where,

$$\boldsymbol{C}(n) = \sum_{k=1}^{n} \lambda^{(n-k)}\boldsymbol{X}(k)\boldsymbol{X}^{\boldsymbol{T}}(k) \tag{7}$$

$$e(n) = d(n) - \boldsymbol{X}^T(n)\boldsymbol{H}(n) \tag{8}$$

$\boldsymbol{C}(n)$ depicts the weighted least squares auto-correlation function, $\boldsymbol{X}(k)\boldsymbol{X}^T(k)$, of the N dimensional input vector $\boldsymbol{X}(n)$.

When updating the RLS algorithm model coefficients as seen in equation 6, the size of $\boldsymbol{C}^{-1}(n)$ is determined by the total number of Volterra model coefficients given a particular memory length and model order of non linearity as defined by equation 1. Increasing the order of non linearity and memory tap length of the Volterra model increases the size of $\boldsymbol{C}^{-1}(n)$, thus eigen decomposition, as utilised in cited related work, can become extremely complex.

Equation 5 of the RLS training algorithm presents that the expected value of $\boldsymbol{C}^{-1}(n)$ is a function of the auto correlation matrix. When examining an isolated sample of the signal, $\boldsymbol{X}_n$, it is treated as a random variable with expected values in the form of $E\{\boldsymbol{X}\boldsymbol{X}^{\boldsymbol{T}}\}$. This is used in equation 7 and expanded in equation 9 to illustrate the behavior of the calculation .

$$\boldsymbol{R}_{xx} = \begin{bmatrix} E[\boldsymbol{X}_1\boldsymbol{X}_1] & E[\boldsymbol{X}_1\boldsymbol{X}_2] & \dots & E[\boldsymbol{X}_1\boldsymbol{X}_n] \\ E[\boldsymbol{X}_2\boldsymbol{X}_1] & \dots & & \vdots \\ \vdots & & & \\ E[\boldsymbol{X}_n\boldsymbol{X}_1] & E[\boldsymbol{X}_n\boldsymbol{X}_2] & \dots & E[\boldsymbol{X}_n\boldsymbol{X}_n] \end{bmatrix} \tag{9}$$

Equation 9 assumes that all of the components are real random vectors. Should the vectors be considered as complex values random vectors $\boldsymbol{R}_{xx}$ must be in Hermitian form [9], which is not realisable in every Volterra model when using various memory and non linear order values.

The model depicted in Figure 1 was of non linear order one, two, three, and seven with a memory length of three. The model error estimate $e(n)$, is given by $e(n) = d(n) - \hat{d}(n)$, where $\hat{d}(n)$ represents the estimated output of the model. The value of $e(n)$ becomes extremely high abruptly at the onset of instability due to the error having reached it's minimum as defined by RLS, resulting in a divergence from the minimum error.

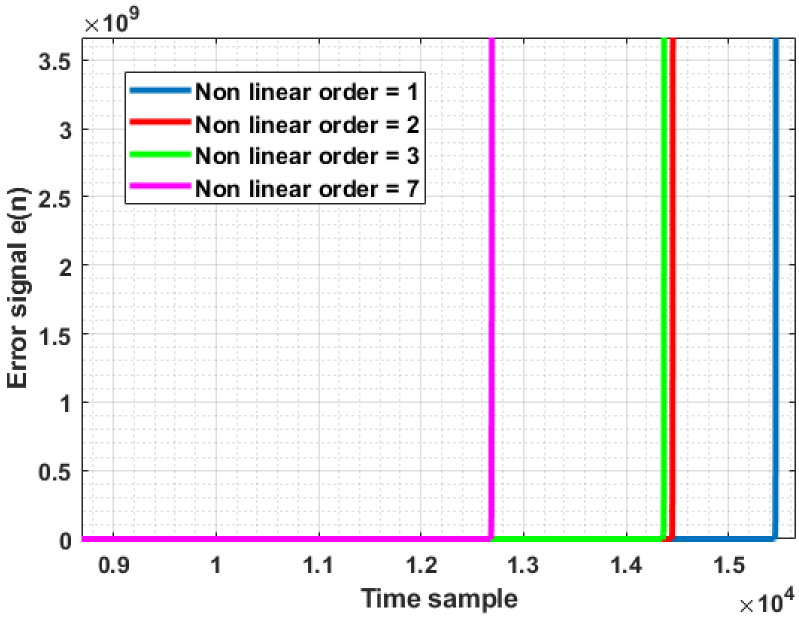

Fig. 1 An illustration of the error signal increasing in magnitude versus time samples of the input training signal. Instability is indicated by a rapid increase in magnitude, as shown for each non linear order of the Volterra model.

Each order of non-linearity encounters the onset of instability at a different time sample for the same dataset. The calculation of minimum error is estimated utilising 9, of different sizes depending on the non linear order of the model as shown in equation 5. Therefore there is a finite input length of training signal $\boldsymbol{X}(n)$ that can be utilised for this model before instability occurs, regardless of the value of non-linear order, memory tap length and sampling frequency.

4 Early stopping criterion

Aforementioned related works focus on improving the NMSE or adding additional computational complexity by altering the RLS algorithm. This manuscript determines a method by which to desist training of a model using RLS before instability occurs. Instability can be circumvented by a simple observation of a value that is pre-existing natively in the conventional RLS algorithm and therefore does not increase computational complexity.

The update matrix as in equation 5 is calculated by the difference of two separate matrix manipulations, with one matrix manipulation containing the more current information of the autocorrelation function, consisting of the right hand side of equation 5. Henceforth, this will be referred to as the change in update matrix and denoted it as $\triangle C^{-1}(n)$, as defined in equation 10. Equation 5 contains an inherent flaw i.e. that a difference equation has the potential to generate eigenvalues that result in a divergence from the trajectory of minimum error [9]. To avoid the estimated output of the model diverging from the least squares error, previous authors have examined eigen analysis of the auto correlation function. This involves altering the limits specified in the auto correlation function based on the statistical analysis of the specific input training signal and, therefore, requiring individual computations for each respective training signal.

$$\triangle C^{-1}(n) = \frac{K(n)\boldsymbol{X}^T(n)\boldsymbol{C}^{-1}(n-1)}{\lambda} \tag{10}$$

As RLS minimises the linear least cost function, the phase $\triangle C^{-1}(n)$ is expected to tend toward the projection of the minimum error with consistent phase, i.e the desired output and actual output are tending toward the same point in the complex plane. Significant deviations in the complex values of $\triangle C^{-1}(n)$ from the original trajectory indicates definitively the onset of instability. The phase of $\triangle C^{-1}(n)$ was chosen as the stopping criterion as it does not add any additional computational complexity.

By observing $\triangle C^{-1}(n)$ on a sample per sample basis it is possible to identify the sample point at which instability begins to occur. As the auto correlation function relates $X(n)$ and $X(n-1)$, which contain $N-1$ common elements, and therefore should remain highly similar to previous values. Observing the first element of the matrix $\triangle C^{-1}(n)$, allows for a comprehensive measurement of the eigen vector behaviour as the diagonal values of $\triangle C^{-1}(n)$ will be identical as seen in equation 9. In this way, a deviation in the sample to sample values in $\triangle C^{-1}(n)$ indicates a deviation from the trajectory towards the minimum error.

Figure 2 depicts how stability may be inferred from the proposed surrogate measure $\triangle C^{-1}(n)$. As previously stated, stability is indicated by the plotted vectors remaining in close proximity to the trajectory of minimum error. A change in direction and sudden increase of the magnitude of the vectors indicates that the estimate $\hat{d}(n)$, is tending away from the plane of the least squares estimation of the error.

While a simulated PA will not introduce any external errors into the model, experimental validation may incur errors such as those resulting from noise contributions. As such it is necessary to introduce a threshold into the early stopping criterion to prevent premature termination of training. The tolerance we suggest is that the phase component of $\triangle C^{-1}(n)$ should fall between ∓ 0.25 Radians. The phase of the $\triangle C^{-1}(n)$ rises rapidly, as can be seen in Figures 3 (a) and 2. Therefore ∓ 0.25 Radians was considered to be a suitable prescribed tolerance as ceasing training prior to an extreme divergence of the phase component allows for the RLS algorithm preserve high fidelity of the estimated output without alteration to the RLS algorithm.

In Figure 2 it can be seen that the model behaviour has become imbalanced i.e. the vectors have exceeded ∓ 0.25 Radians prescribed tolerance. Once the point of convergence, or minimum error, is exceeded the eigen vectors are becoming oscillatory and increase in magnitude, i.e. attempting to point in the direction of largest variance, ∞ [17]. Therefore, it is beneficial to cease training once the point of convergence has been exceeded as defined by the prescribed threshold that is applied to the resulting surrogate measure obtained from the first value of the matrix given by equation 9.

5 Experimental validation

In order to validate the early stopping criteria proposed in this work a variety of single carrier signals are sent from an AD-FMCOMMS3 evaluation board, through a Doherty PA at 2.6GHz. The corresponding input and output signals are sampled at 30.72 MHz. To illustrate the onset of instability an arbitrary memory length and order of non linearity was tested. For the purposes of illustration both values were set to 2 producing Figure 3. Each of the four modulation schemes become unstable at different time samples (n) as seen in 3 (a). DVBS2x

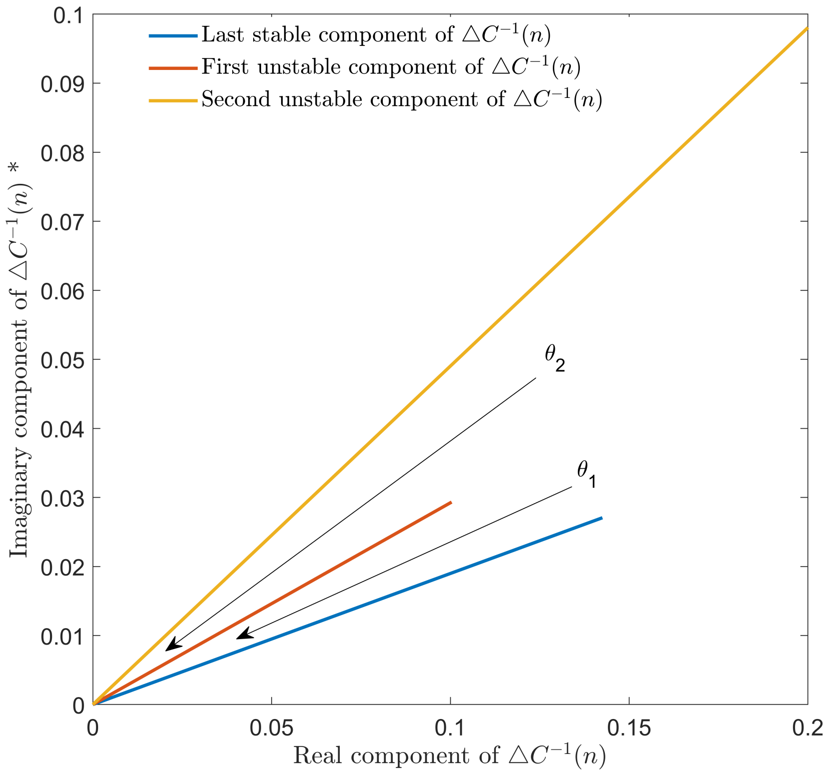

Fig. 2 Illustration of phase discrepancy, of $\triangle C^{-1}(n)$. θ_1 depicts the phase of the first complex value of $\triangle C^{-1}(n)$ is 0.1876 Radians. θ_2 is 0.5278 Radians
* The limits of this figure have been truncated for aesthetic purposes. Please note the magnitude of the second unstable $\triangle C^{-1}(n)$ extends to co-ordinates 0.5891 + 0.2888i

becomes unstable at n= 1.3742×10^4, WCDMA becomes unstable at n=1.385×10^4, 5G NR becomes unstable at n =1.425×10^4 and OFDM LTE becomes unstable at n = 1.428×10^4.

Figure 3 (b), plots the experimentally validated output of the PA versus the estimated output of the PA model utilising the proposed algorithm. The early stopping criterion algorithm ceased training prior to instability as defined by the phase contained by the first complex value of $\triangle C^{-1}(n) > 0.25$ Radians. Both estimated outputs were compared to the experimentally validated output in terms of the Normalised Mean Square Error (NMSE) as illustrated by Table 1.

Figure 4 illustrates the onset of instability with regard to the phase, imaginary and real component of $\triangle C^{-1}(n)$. The imaginary and phase components of the first element of $\triangle C^{-1}(n)$ diverge by a large amount close the point of onset of instability.

The model utilising the proposed algorithm returned acceptable model accuracy in terms of NMSE values, as seen in Table 1. The NMSE values listed in the table show that, by utilising the early stopping criterion, the NMSE value indicates high fidelity between the estimated output and the actual output (visually illustrated in Figure 5). Severe degradation

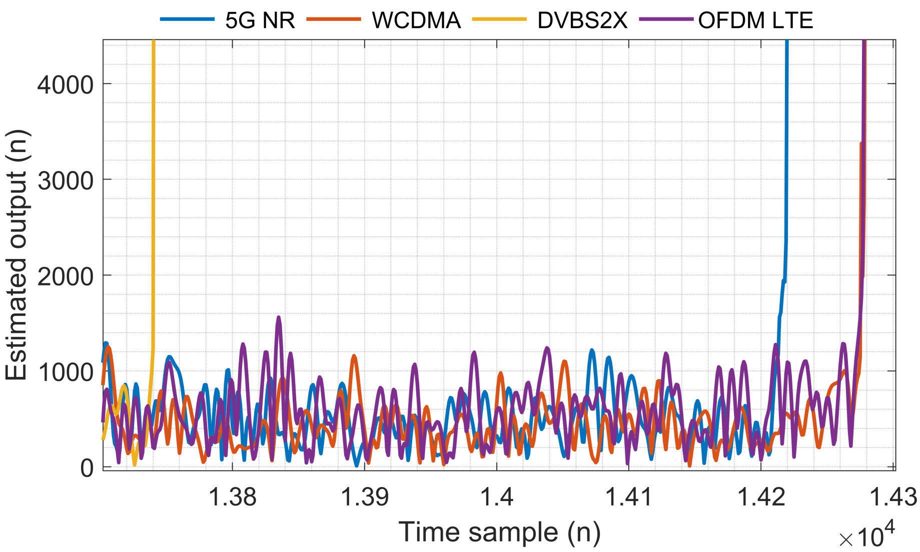

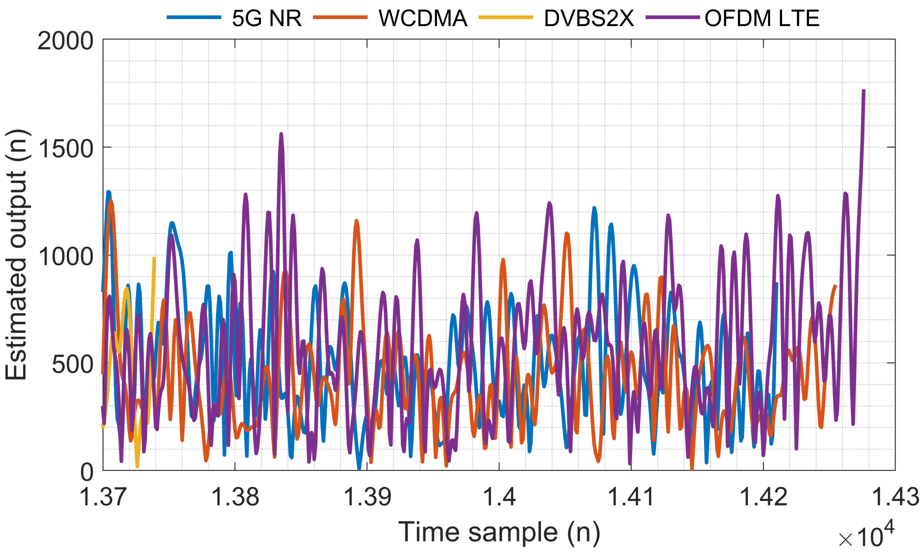

Fig. 3 Experimentally validated output signal (a) estimated signal output without early stopping criterion and (b) with proposed early stopping criterion. It can be seen in (b) that the input training signal length has been truncated prior to the onset of instability. Let it be noted that for illustrative purposes only samples from 13700 onwards are depicted

of the NMSE values occurs rapidly after this point, as shown by the NMSE values listed for +10 and +20 samples after the early stopping criterion recommends the cessation of training. Not only will the early stopping criteria prevent the training routine producing unstable outputs, but it will also maximise the length of the input training signal. Therefore allowing the continued reduction of the model coefficient error, maximising the accuracy of the extracted model.

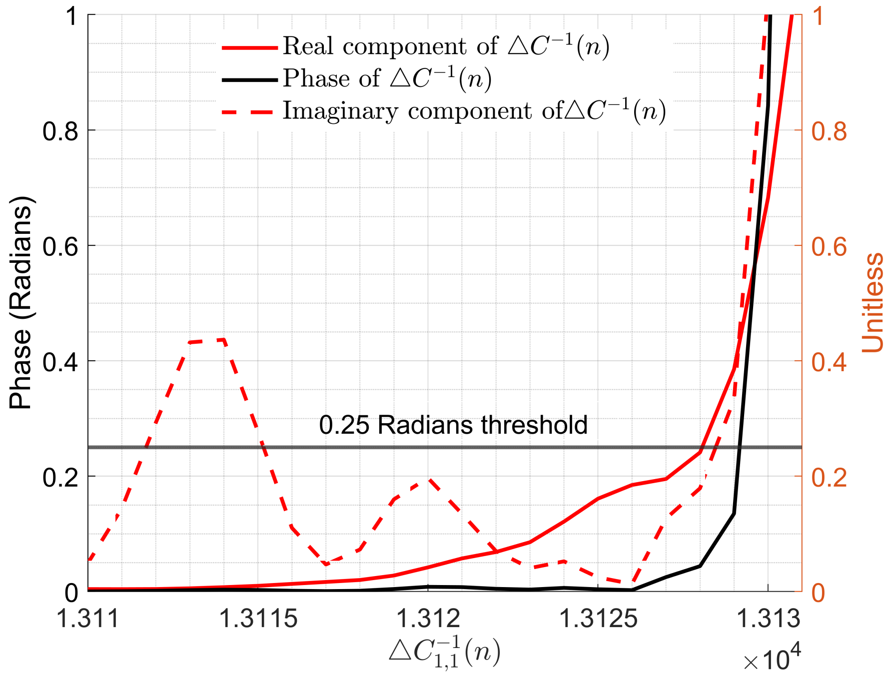

Fig. 4 Real, Imaginary and Phase components of the change in update matrix, $\triangle C^{-1}(n)$, as the early stopping criterion is surpassed. The early stopping criterion is shown as a constant 0.25 Radians threshold that indicates instability when exceeded by the phase. Phase was chosen rather than the real or imaginary components as the indicating factor in order to maximise the input training signal length. Let it be noted the limits of this figure have been truncated for aesthetic purposes

Autonomous control of the stopping criteria removes the possibility of experimental error through heuristic approaches. Let it be noted that this experiment was conducted with various non linear orders and memory lengths. The early stopping criteria operated as expected for all values, including memory lengths and non linear orders of disparate values. As expected from Figure 1, the input training signal length approached instability earlier as the memory lengths and non linear orders increased.

Figure 5, plots the experimentally validated output of the model trained with distinct signal standards versus the estimated output of the model using the proposed algorithm. All signals were 5MHz bandwidth single carrier signals sent through a Doherty PA at 2.6GHz, the same experimental procedure as mentioned above.

The NMSE values shown in Table 1 for the various signal standards each show a distinct improvement where the early stopping criterion has been implemented. Three of four signals NMSE values dis-improve marginally up to ten time samples after the early stopping criterion is met. However, twenty time samples after the early stopping criterion is met, the extracted model NMSE values have dramatically degraded in all four cases. The NMSE values in Table 1 indicate that, through the application of the proposed early stopping criterion, training is terminated prior to instability occurring. This does not require alteration of the RLS algorithm rather a monitoring of a single value that is inherent to the calculation.

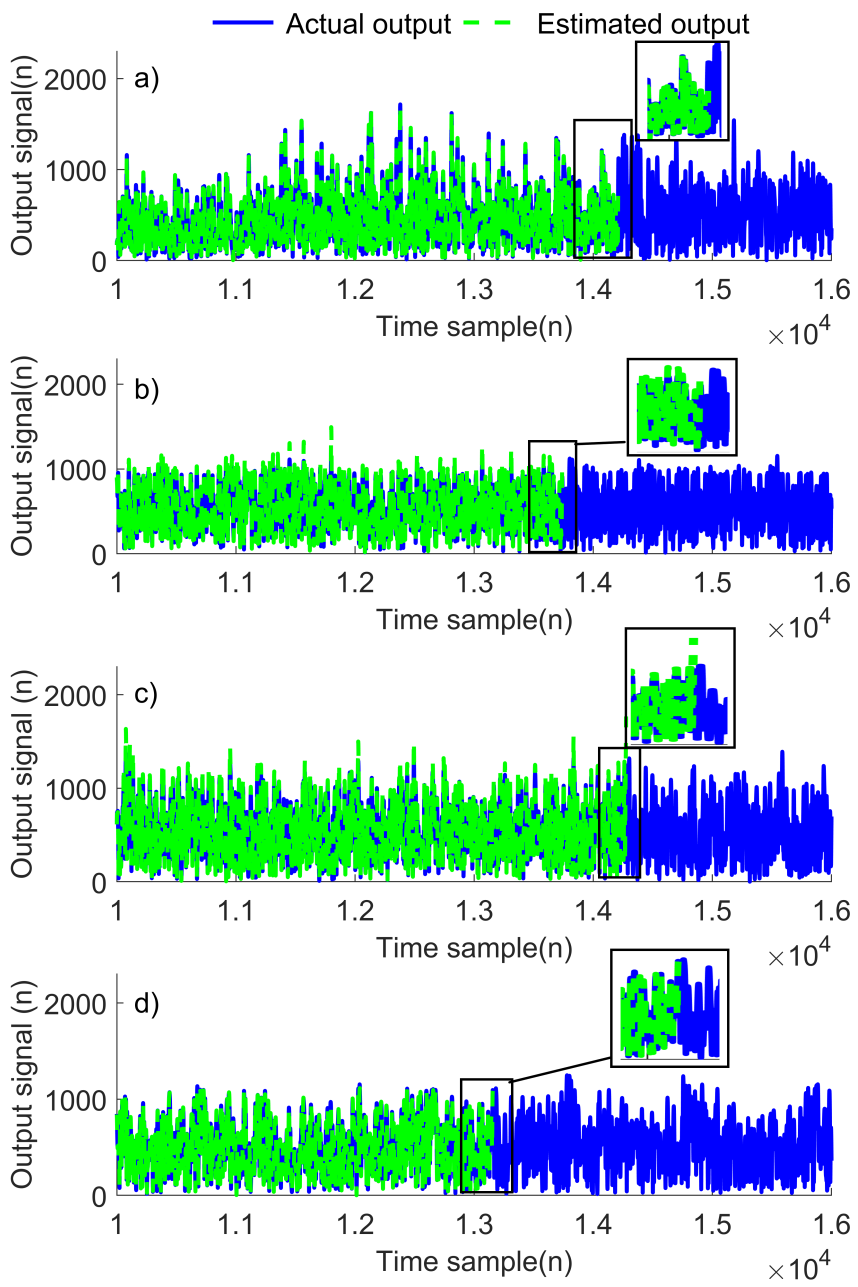

Fig. 5 Experimental signal output versus estimated signal output of various signal standards with proposed algorithm (a) 5G-NR, (b)DVBS2X, (c)LTE OFDM and (d) WCDMA.In each of these cases it can be seen that the estimated output corresponds closely with the experimentally validated output, indicating that the applied algorithm does not negatively affect the modeling capabilities. Zoomed in sections have been provided for clarity. Let it be noted that for illustrative purposes only samples from 10^3 onwards are depicted

Table 1 A comparison of NMSE values when stopped using early stopping criterion(ESC), 10 samples beyond ESC, 20 samples beyond ESC

Signal Standard	ESC	ESC+10	ESC + 20
WCDMA	**-25.514 dB**	**-24.737 dB**	**5.286 dB**
DVBS2X	**-25.427 dB**	**-14.459 dB**	**14.941 dB**
LTE OFDM	**-24.904 dB**	**-24.903 dB**	**4.118 dB**
5G-NR	**-24.4079 dB**	**-23.615 dB**	**-3.136 dB**

6 Conclusion

In conclusion, this paper provides an early stopping criterion to avoid the onset of instability of a Volterra model during RLS training. Experimental validation of the proposed procedure shows that the NMSE of the experimental output vs estimated output indicates high fidelity until the training instance identified by the early stopping criterion is exceeded and then it deteriorates rapidly. NMSE values are detailed in Table 1 and visually illustrated by Figures 3, 2 and 4. Application of this early stopping procedure eliminates the need to apply supplementary computational analysis, thereby minimising the computational complexity required to guarantee a stable model while maintaining it's accuracy. Automating this early stopping procedure is conveniently implemented, only requiring the observation of a pre-existing value that is produced by the RLS algorithm. This method has been experimentally validated for a high power amplifier using four signal standards namely LTE OFDM, WCDMA, DVBS2X and 5G-NR.

Declarations

This publication has emanated from research conducted with the financial support of Science Foundation Ireland (SFI) and is co-funded under the European Regional Development Fund under Grant Number 13/RC/2077.

The authors declare they do not have any conflict of interests / competing interests.

Availability of data and material, not applicable.

Code availability, not applicable.

References

1. K. Zheng, Z. Yang, K. Zhang, P. Chatzimisios, K. Yang, W. Xiang, IEEE Network **30**(1), 44 (2016). DOI 10.1109/MNET.2016.7389830
2. J. Kral, T. Gothans, R. Marsalek, M. Harvanek, in *2018 25th International Conference on Telecommunications (ICT)* (2018), pp. 471–475
3. J. Kral, T. Gotthans, M. Harvanek, in *2017 27th International Conference Radioelektronika (RADIOELEKTRONIKA)* (2017), pp. 1–5
4. J.C. Pedro, S.A. Maas, IEEE Transactions on Microwave Theory and Techniques **53**(4), 1150 (2005). DOI 10.1109/TMTT.2005.845723
5. Changsoo Eun, E.J. Powers, IEEE Transactions on Signal Processing **45**(1), 223 (1997). DOI 10.1109/78.552219
6. M. Hoflehner, A. Springer, in *Computer Aided Systems Theory – EUROCAST 2011*, ed. by R. Moreno-Díaz, F. Pichler, A. Quesada-Arencibia (Springer Berlin Heidelberg, Berlin, Heidelberg, 2012), pp. 9–16
7. S. Rahmanian, M. Bateni, E. Yazdian, Circuits, Systems, and Signal Processing **39** (2020). DOI 10.1007/s00034-020-01423-9
8. J. Ren, IEEE Access **PP**, 1 (2020). DOI 10.1109/ACCESS.2020.2976152
9. V.J. Mathews, G.L. Sicuranza, *Polynomial signal processing* (Wiley, 2000)

10. J.N. Swaminathan, P. Kumar, Wireless Personal Communications **90**(2), 807 (2016). DOI 10.1007/s11277-016-3217-9
11. R. Schumacher, E.G. Lima, G.H. Oliveira, Circuits, Systems, and Signal Processing **35**(7), 2298 (2016). DOI 10.1007/s00034-015-0151-0
12. R.N. Braithwaite, in *2019 IEEE Topical Conference on RF/Microwave Power Amplifiers for Radio and Wireless Applications (PAWR)* (2019), pp. 1–3. DOI 10.1109/PAWR.2019.8708729
13. S. Moghaddamnia, M. Fuhrwerk, J. Peissig, in *2018 15th International Symposium on Wireless Communication Systems (ISWCS)* (2018), pp. 1–6. DOI 10.1109/ISWCS.2018.8491222
14. Z. Jiang, J. Wang, W. Wu, in *Proceedings of the 2nd International Conference on Telecommunications and Communication Engineering* (Association for Computing Machinery, New York, NY, USA, 2018), ICTCE 2018, p. 167170. DOI 10.1145/3291842.3291848. URL https://doi.org/10.1145/3291842.3291848
15. P. Varahram, S. Mohammady, R. Farrell, J. Dooley, Wireless Personal Communications **112**(2), 651 (2020). DOI 10.1007/s11277-020-07066-y. URL https://doi.org/10.1007/s11277-020-07066-y
16. A. Zhu, J. Dooley, T.J. Brazil, in *2006 IEEE MTT-S International Microwave Symposium Digest* (2006), pp. 1113–1116. DOI 10.1109/MWSYM.2006.249958
17. B. Farhang-Boroujeny, *Adaptive Filters: Theory and Applications, 2nd Edition* (John Wiley Sons, 2013)

Figures

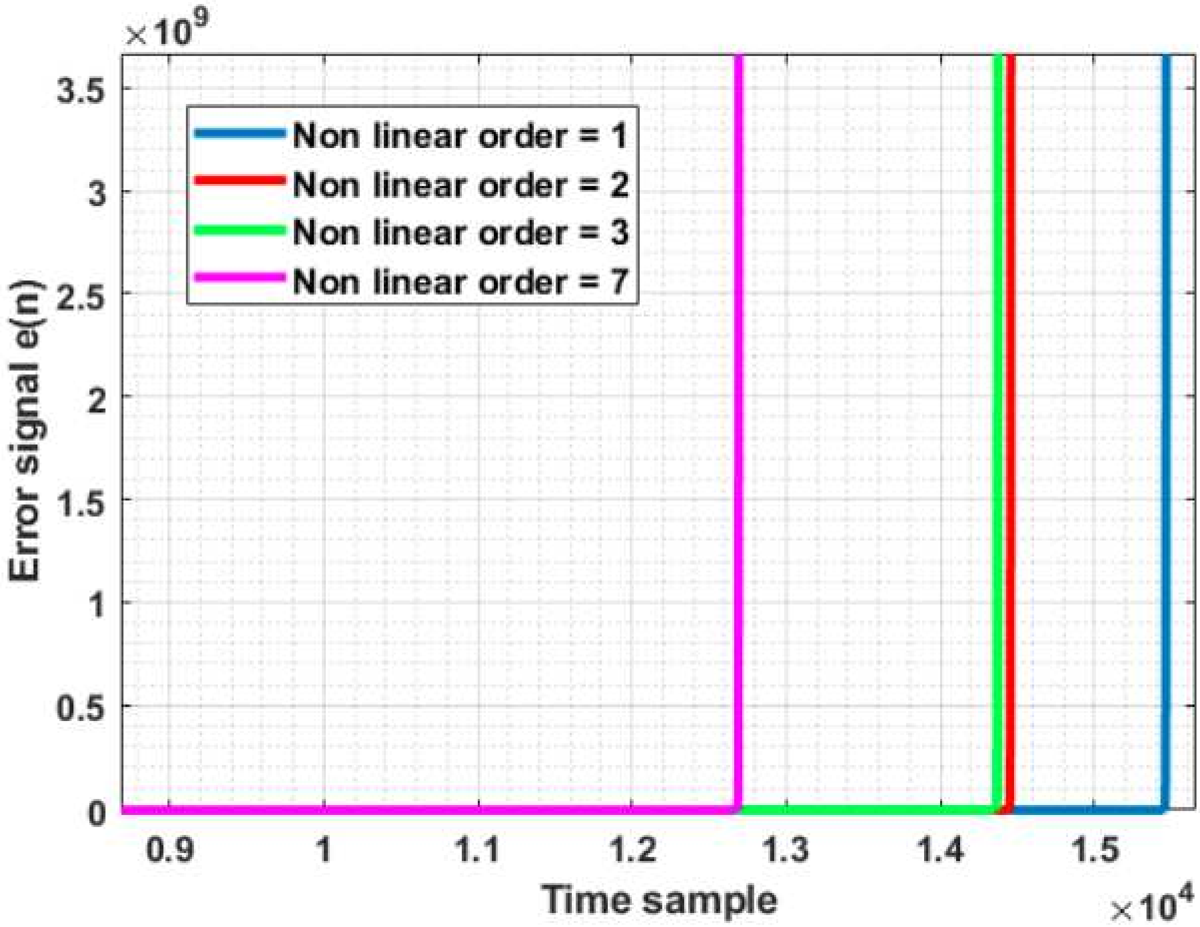

Figure 1

Please see the Manuscript PDF file for the complete figure caption

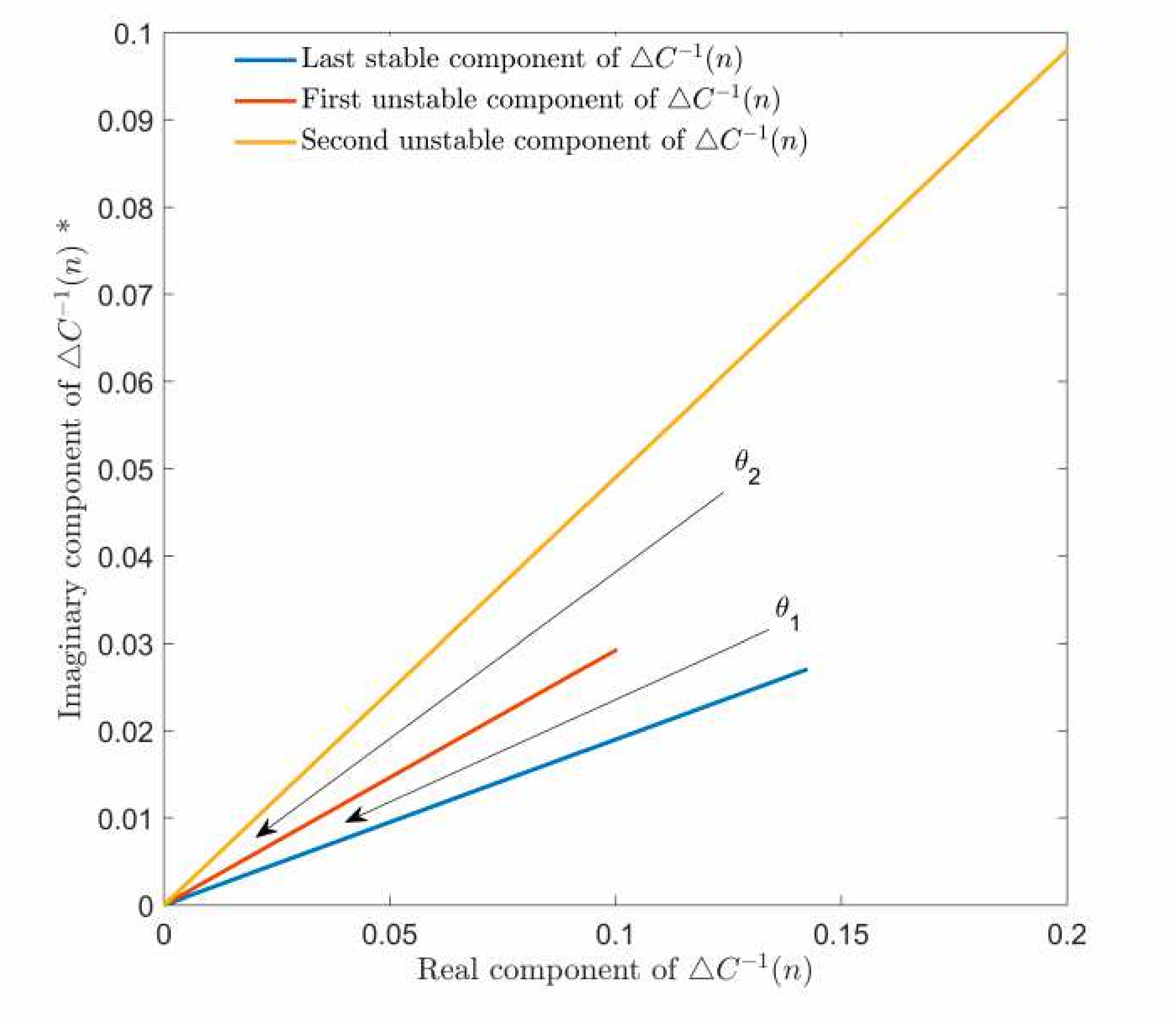

Figure 2

Please see the Manuscript PDF file for the complete figure caption

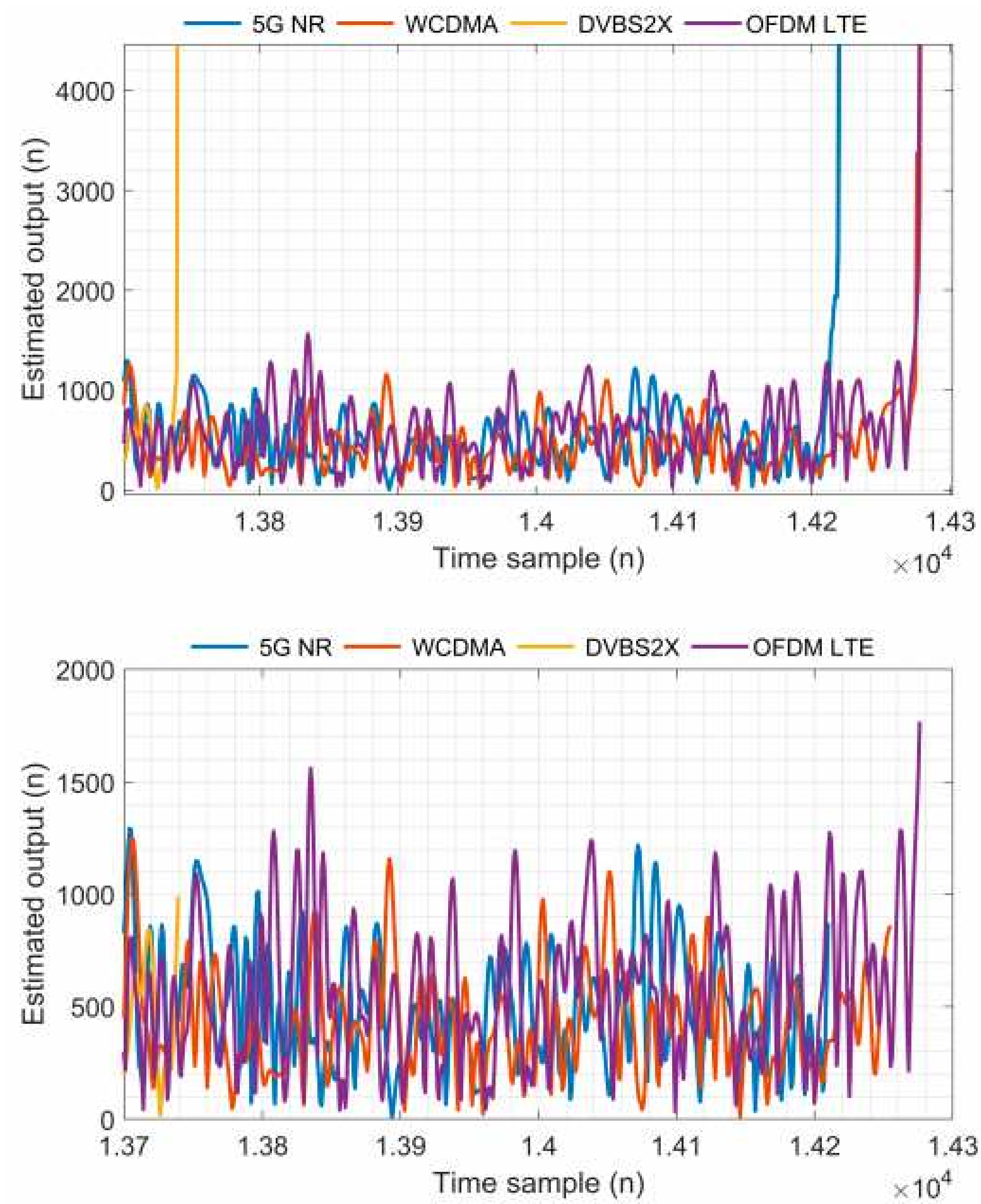

Figure 3

Please see the Manuscript PDF file for the complete figure caption

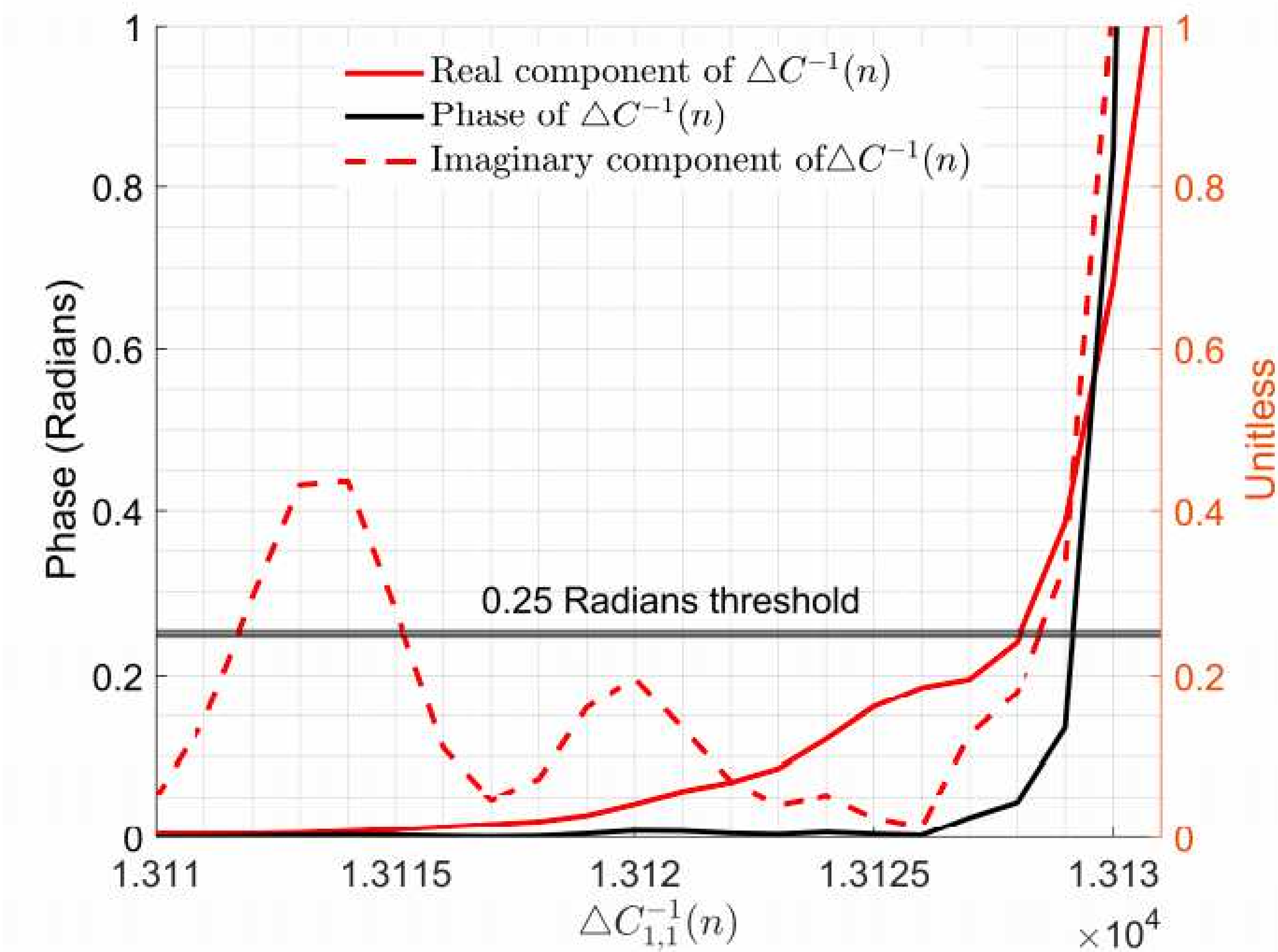

Figure 4

Please see the Manuscript PDF file for the complete figure caption

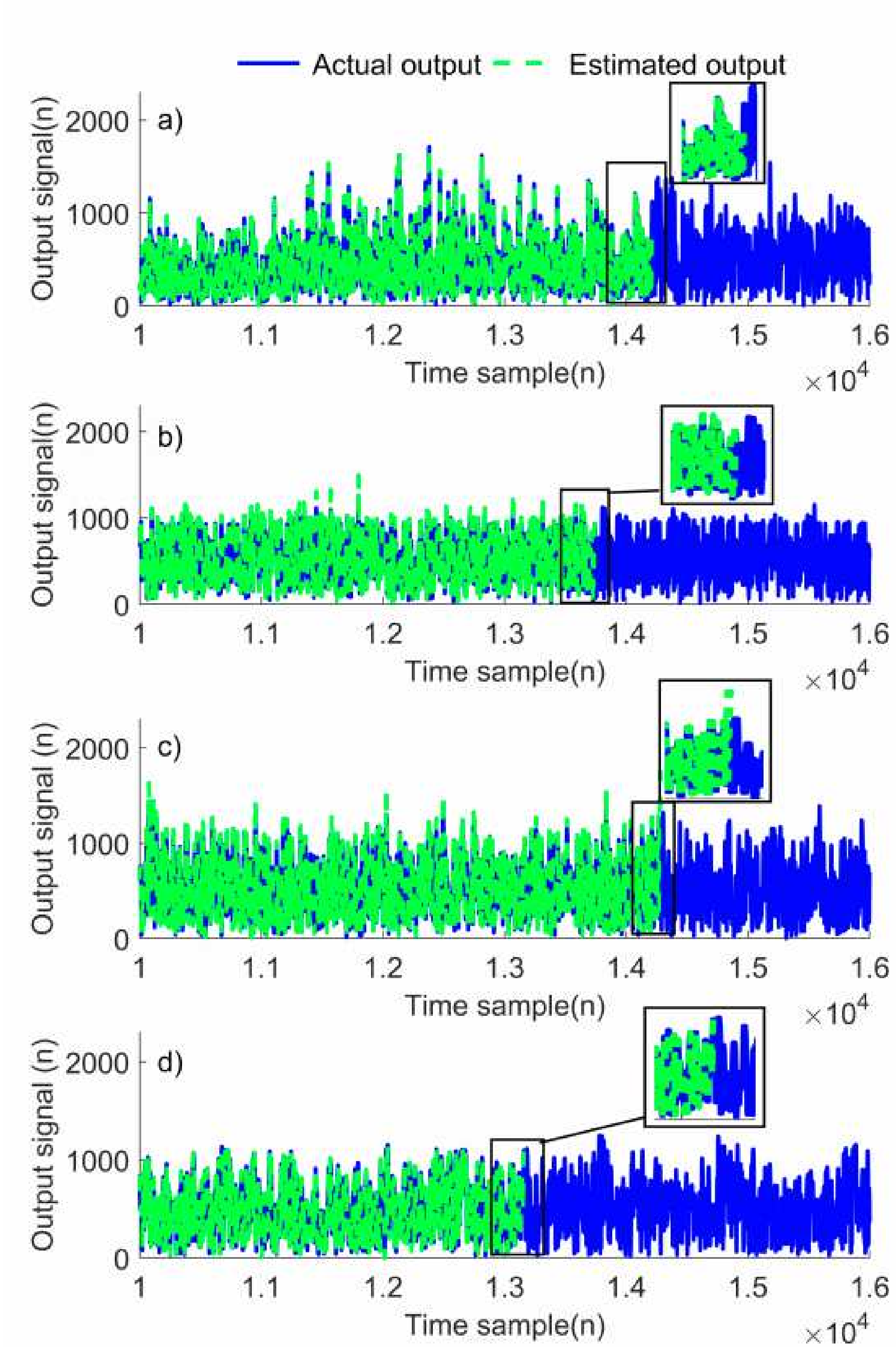

Figure 5

Please see the Manuscript PDF file for the complete figure caption